Dynamics of Rydberg wave packets generated by half-cycle pulses

C. O. Reinhold and J. Burgdörfer

Physics Division, Oak Ridge National Laboratory, Oak Ridge, Tennessee 37831-6373
and Department of Physics and Astronomy, University of Tennessee, Knoxville, Tennessee 37996-1200

M. T. Frey and F. B. Dunning

Department of Physics and the Rice Quantum Institute, Rice University, 6100 South Main Street, Houston, Texas 77005-1892

Wave packets comprising a superposition of very-high-lying Rydberg states have been created using a half-cycle pulse (HCP). The properties of the wave packet are probed using a second HCP that is applied following a variable time delay. The second pulse ionizes a fraction of the atoms and the survival probability exhibits pronounced oscillations that are associated with the quasiperiodic evolution of the wave packet. Good agreement is found between the experimental data and the results of a classical trajectory Monte Carlo simulation demonstrating that, for the times investigated, classical-quantum correspondence holds and quantum corrections are negligible. [S1050-2947(96)51007-3]

In recent years there has been increasing effort devoted to the study of nonstationary states formed from a coherent superposition of nearby high-n Rydberg states. Such Rydberg wave packets have been created by photoexcitation of ground-state atoms using ultrashort laser pulses whose bandwidth exceeds the level spacing in the final Rydberg manifold [1–3] and are of interest because they frequently display novel dynamical behavior. Since photon absorption occurs when the electron is close to the core ion, the wave packet is initially strongly localized in the vicinity of the core. As time advances, the wave packet expands and contracts radially very much like a classical particle in a Kepler orbit. This behavior is then monitored using a second ultrafast probe pulse.

Here we discuss an alternate approach to the generation of Rydberg wave packets: excitation from a single (stationary) initial Rydberg state, with principal quantum number n_i, using a so-called "half-cycle pulse" (HCP). A HCP [4–10] comprises a strong unidirectional electric field $\vec{F}(t)$ whose duration, T_p, can be much shorter than the classical electron orbital period, T_{n_i}, associated with the initial state. The wave packet produced by such a HCP differs significantly from that generated by an ultrashort laser pulse because the integral of the applied electric field is finite. In the limit of very short HCPs, $(T_0 = T_p/T_{n_i} \ll 1)$, the HCP simply delivers an impulsive momentum transfer,

$$\Delta \vec{p} = -\int_{-\infty}^{\infty} \vec{F}(t)dt, \qquad (1)$$

to the excited electron (atomic units are used throughout). Such momentum transfer leads directly to excitation to higher-lying states and can, for sufficiently strong pulses, even induce ionization. The evolution of the wave packet formed by the HCP is analyzed using a second HCP that is applied after a variable delay. Experimental studies using potassium Rydberg atoms reveal quasiperiodic behavior of the wave packet that can be reproduced using classical trajectory Monte Carlo (CTMC) calculations without need of

any adjustable parameters. The data demonstrate that the study of wave-packet dynamics provides an excellent tool to probe the transition between quantum and classical behavior of atomic systems. On general grounds [11], one expects the quantum and the classical evolution to depart from each other at a characteristic "break" time $t_c \simeq 2\pi/\Delta E$, where ΔE is the smallest level spacing. For Rydberg states, the level spacing $E_{n+1} - E_n = n^{-3}$ and t_c corresponds to the classical Kepler orbital period $T_n = 2\pi n^3$. As will be shown below, for a wave packet in the Coulomb-Kepler problem the break time exceeds T_n; i.e., the classical evolution can mimic the quantum evolution beyond T_n.

The apparatus used in the present experiment is described in detail elsewhere [5,12]. Briefly, K(np) Rydberg atoms are created by photoexciting ground-state potassium atoms in a thermal-energy beam using a frequency-doubled Coherent CR 699-21 dye laser. Excitation occurs near the center of an interaction region defined by three pairs of planar electrodes that are biased to locally reduce stray electric fields to $\lesssim 50$ μV cm^{-1}. The HCPs are created by applying voltage pulses to a circular copper disk that is inset in the upper electrode. The pulses used in the present work were of ~ 2 ns duration and were produced using an Avtech model AVI-V pulse generator. The output of the generator is split into two pulses of approximately equal amplitude by a matched resistive power divider. One of the resulting pulses is delayed using a length of RG402 cable and the two pulses are then recombined using a matched power combiner and transported to the HCP electrode by rigid coaxial cable. The individual pulses can be attenuated and/or inverted by connecting fixed broadband attenuators and/or an inverting pulse transformer in series. The pulse shapes and amplitudes at the HCP electrode are directly measured using a fast probe and sampling oscilloscope. Spatial variations in the field produced by the HCP electrode, and uncertainties inherent in the measurement of the HCP amplitude, introduce a small uncertainty, $\lesssim \pm 10\%$, in the applied fields.

Measurements are conducted in a pulsed mode. The laser output is formed into a train of pulses of ~ 4 μs duration
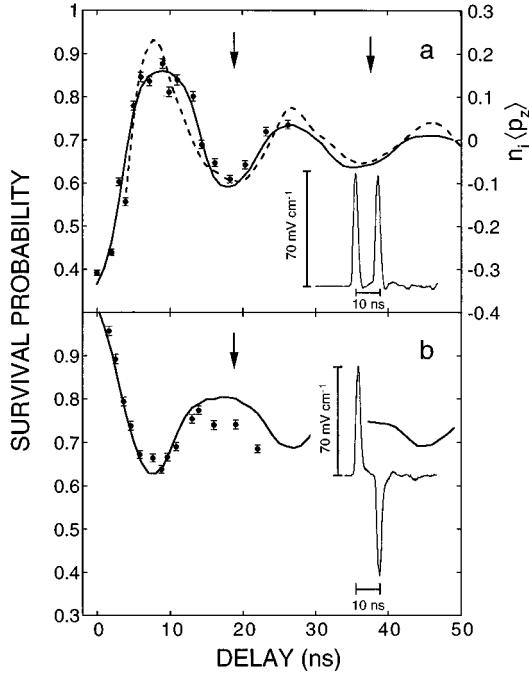
FIG. 1. Rydberg atom survival probability (left scale) following application of two HCPs in (a) the same and (b) opposite senses to K($n_i p$) atoms with $n_i \sim 417$ as a function of time delay. ●, experimental data; —, results of CTMC calculations. Multiples of T_{n_f} are marked by arrows. The insets show the pulse profiles. --- (right scale), time development of the scaled expectation value $\langle p_z \rangle / p_{n_i} = n_i \langle p_z \rangle$ following application of the first HCP.

with a pulse repetition frequency of $\sim$10 kHz. (The probability that a Rydberg atom is formed during any pulse is small, $\lesssim$0.01, and data are accumulated following many laser pulses.) Excitation occurs in (near) zero electric field. Approximately 200 ns after the end of the laser pulse the HCPs are applied. The surviving Rydberg atoms are then detected by field ionization. Measurements in which no HCPs are applied are interspersed at routine intervals during data acquisition to monitor the number of Rydberg atoms initially produced by the laser. The Rydberg atom survival probability is obtained by comparing the Rydberg atom signals observed with and without HCPs present.

Typical data obtained using parent K($n_i p$) atoms with $n_i \sim 417$ are presented in Fig. 1, which shows the measured survival probability as a function of time delay between the two HCPs. (The error bars indicate only the statistical uncertainties and do not include possible systematic errors associated with uncertainties in the applied field amplitude.) The pulse sequences used are shown in the insets and results are included for the cases where the two pulses are in both the same and opposite senses. The pulse amplitudes were selected to achieve survival probabilities of $\sim$0.6 and correspond to a scaled momentum transfer $\Delta p_0 = \Delta p / p_{n_i} = 0.53$. A pronounced quasiperiodic dependence of the survival probability on delay time is observed that can be explained by considering the time evolution of the wave packet created by the first HCP.
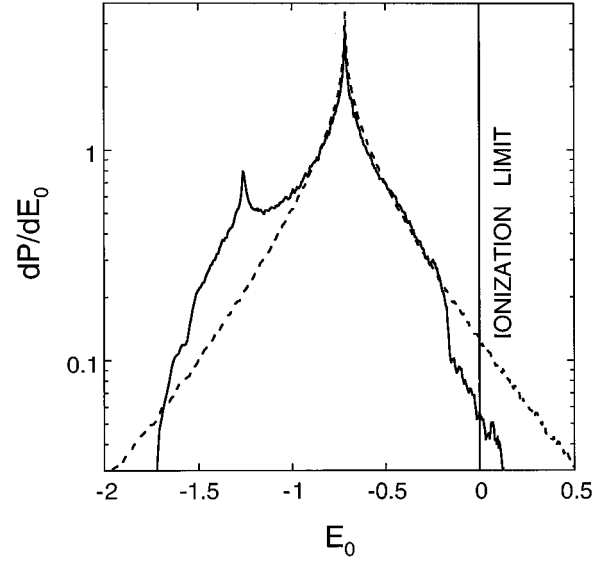

FIG. 2. Final-state energy distribution following application of a HCP to hydrogen atoms in the 417p state: ---, ultrashort HCP ($T_p / T_{n_i} = 0$); —, a pulse of 2 ns duration ($T_p / T_{n_i} = 0.18$). The scaled momentum transfer $\Delta p_0 = \Delta p / p_{n_i} = 0.53$. The energy axis is scaled to the energy of the initial state, i.e., $E_0 = E / |E_{n_i}|$.

If the atom is initially in some stationary Rydberg state $|\phi_i\rangle$, the electronic wave function immediately after application of the HCP may be written $|\Psi(t=0)\rangle = |\phi_i^B\rangle = e^{i \Delta \vec{p} \cdot \vec{r}} |\phi_i\rangle$ and corresponds to the initial state shifted in momentum space by $\Delta \vec{p}$. The corresponding expectation values of the energy and momentum are

$$\langle E \rangle_{t=0} = \langle \phi_i^B | H_{\mathrm{at}} | \phi_i^B \rangle = \langle \phi_i | H_{\mathrm{at}} | \phi_i \rangle + \frac{(\Delta p)^2}{2}$$
$$+ \langle \phi_i | \vec{p} \cdot \Delta \vec{p} | \phi_i \rangle, \qquad (2)$$

$$\langle \vec{p} \rangle_{t=0} = \langle \phi_i^B | \vec{p} | \phi_i^B \rangle = \Delta \vec{p} + \langle \phi_i | \vec{p} | \phi_i \rangle, \qquad (3)$$

where H_{at} is the atomic Hamiltonian and $\vec{r}$ and $\vec{p}$ are the electron position and momentum operators, respectively. Note that $\langle nlm | \vec{p} | nlm \rangle = 0$ and, therefore, $\langle E \rangle_{t=0} = E_{n_i} + (\Delta p)^2/2$, where E_{n_i} is the energy of the initial Rydberg state. Classically, the application of a HCP to an electron with momentum $\vec{p}$ and energy E_{n_i} changes its energy to $E(t=0) = E_{n_i} + [(\Delta p)^2/2] + \vec{p} \cdot \Delta \vec{p}$. The classical average of E over an ensemble of phase-space points representing the initial quantum state $|\phi_i\rangle$ agrees with the quantum-mechanical result.

The final electronic wave function can be expanded as

$$|\Psi(t)\rangle \simeq \sum_n e^{-iE_n t} \sum_l \langle nlm | \Psi(0)\rangle |nlm\rangle \qquad (4)$$

and encompasses a broad distribution of angular momentum states, including high-l states. We choose a quantization z axis in the direction of the HCP and, therefore, m is a constant of the motion. The HCP leads to population of a range of higher-n states centered around $n_f = \sqrt{-2\langle E \rangle_{t=0}}$. Figure 2

shows the excitation function (or energy distribution), calculated using CTMC techniques, associated with application of a HCP to hydrogen atoms in the $n_i=417$, $l_i=1$ state. The scaled momentum transfer is equal to that for the data in Fig. 1, i.e., $\Delta p_0/p_{n_i}=0.53$, and calculations are included for both an ultrashort pulse ($T_p/T_{n_i}=0$) and a pulse of ~ 2 ns duration ($T_p/T_{n_i}=0.18$) as used in the experiments. The final-state distribution is peaked about the expectation value given by Eq. (2), which corresponds to $n_f \sim 493$, and has a "width" that encompasses a range of n values Δn of $\Delta n \sim 20$. For HCPs of finite duration, a small secondary peak is also evident in the final-state distribution at energies corresponding to $n_f < n_i$, and the likelihood of direct ionization is somewhat decreased.

The time evolution of the wave packet can be understood classically by considering the time development of the expectation value of the z component, p_z, of momentum of the exited electron following HCP application. Initially the HCP imparts net momentum to the electron in the $-z$ direction, i.e., $\langle p_z \rangle < 0$. CTMC calculations show that after approximately one-half of the mean orbital period T_{n_f} associated with the final-state distribution, quasiclassical "orbital" motion of the electron leads to a peak in the p_z distribution at positive p_z, i.e., $\langle p_z \rangle > 0$. As orbital motion continues, the distribution once more becomes strongly peaked at negative p_z. This cycle then repeats and, as illustrated in Fig. 1, continued orbital motion causes $\langle p_z \rangle$ to oscillate between negative and positive values with period $\sim T_{n_f}$. The amplitude of the oscillation decreases steadily with time, however, because a distribution of final states is excited that evolve differently in time leading to dephasing.

Consider now the effect of applying a second half-cycle probe pulse (again along the z axis) to the wave packet. If the impulse delivered by the probe pulse is in the same direction as the initial electron momentum, i.e., $\langle p_z \rangle$, the electron momentum (and energy) will be increased. This can lead to ionization and a low survival probability. If, however, the impulse and initial electron momentum are in opposite directions, the final momentum (and energy) of the electron will be lower and the likelihood of survival higher. Thus, if the two pulses are both in the same sense (and impart a negative impulse), the survival probability will be smallest (largest) at delay times such that $\langle p_z \rangle < 0$ (>0). The reverse is true if the probe pulse is in the opposite sense to the initial HCP [see Fig. 1(b)]. The structure evident in Fig. 1 therefore reflects directly the time development of the wave packet, i.e., $\langle p_z \rangle$.

Survival probabilities determined using the CTMC method are included in Fig. 1. These calculations employ the experimentally measured pulse profiles and take into account the presence of small residual fields in the interaction region that ionize states with $n \gtrsim 1200$. Interestingly, survival probability calculations for hydrogen and potassium were found to be indistinguishable. This results because the electron in its initial state spends the bulk of its time well removed from the core ion and because the first HCP populates predominantly high-l states. The CTMC calculations are in very good agreement with the experimental data without use of any adjustable parameters. Figure 3 illustrates, for parent K($n_i p$) atoms with $n_i \sim 417$, the effect of applying sequential
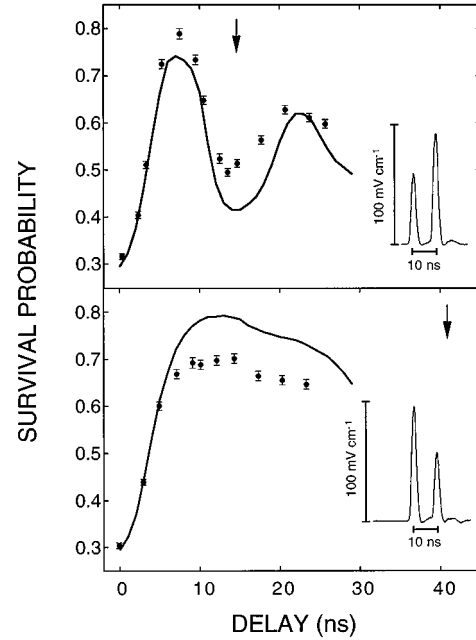

FIG. 3. Rydberg atom survival probability following application of two HCPs of different amplitudes to K($n_i p$) atoms with $n_i \sim 417$. ●, experimental data; —, results of CTMC calculations. The pulse profiles are shown in the insets and the arrows mark T_{n_f}.

HCPs of different amplitudes. The pulse amplitudes, indicated in the insets, were again selected to obtain survival probabilities of ~ 0.6. The results of CTMC calculations are also included and are in very good agreement with the experimental data. As the amplitude of the first HCP increases the time period of the oscillation in the survival probability also increases. This results because larger initial HCP amplitudes populate higher-lying states whose time evolution is slower.

The very good agreement between theory and experiment demonstrates that classical dynamics can reproduce the "quantum beats" observed in the data and moreover that the classical evolution mimics the quantum evolution for times well beyond t_c. This remarkable extended classical-quantum correspondence can be traced to the particular properties of the Coulomb-Kepler problem and of the HCP-generated wave packets. The energy differences in the Rydberg series determining quantum beats are given to second order in $\delta n/n_f$ by

$$E_{n_f+\delta n} - E_{n_f} \simeq \delta n\, \omega_{n_f}\left[1 - \frac{3}{2}\frac{\delta n}{n_f} + 2\left(\frac{\delta n}{n_f}\right)^2\right], \qquad (5)$$

where $|\delta_n| \leq \Delta n/2$. To leading order, the spectrum compares locally to that of a harmonic quantum oscillator, with $\omega_{n_f} = 2\pi/T_{n_f}$ being the *classical* orbital frequency. For a harmonic oscillator, quantum and classical expectation values agree [13], which explains the presence in the classical simulation of beats with the mean orbital period. The damping of the beats is caused by the "anharmonic" correction. Dephas-

ing (by π) or damping occurs over a time $t_D \simeq 4n_f/3(\Delta n)^2 T_{n_f} \simeq 2T_{n_f}$, in agreement with the observations. The fact that classical dynamics can accurately reproduce even the dephasing results because, when Δn is large, the approximation of a large but discrete set by a continuous distribution is valid. Classical dynamics will fail, however, at times approaching the revival time t_R of the wave packet. Complete revival requires $t_R \simeq (n_f/3)T_{n_f}$ [1] which, for the values of n_f of interest here, is quite long and out of reach of the experiment.

Figure 4 shows expectation values $\langle p_z \rangle$ calculated using both classical and quantum methods following application of an ultrashort pulse providing momentum transfer $\Delta p/p_{n_i}=0.53$ to hydrogen atoms initially in the $n_i=100$, $l_i=0$ state. $n_i \approx 100$ ($n_f \approx 118$) is currently our upper limit for which the necessary matrix elements [Eq. (4)] can be computed with sufficient accuracy. The width of the band used for the figure is $\Delta n=16$. The classical and quantum results agree up to $\simeq 6T_{n_f}$, i.e., six times the quantum break time t_c. Classical-quantum correspondence breaks down completely for longer times where revivals occur which are absent in classical dynamics. Such revivals have been observed in HCP studies at $n \sim 25$ [14]. Revival of the wave packet can be treated semiclassically.

In summary, the present work demonstrates that very-high-n Rydberg wave packets can be created and probed using HCPs. The motion of the wave packet is quasiperiodic with a period that can be directly measured. The very good agreement between theory and experiment demonstrates that, for the range of times studied experimentally, classical-quantum correspondence holds and quantum corrections are negligible.
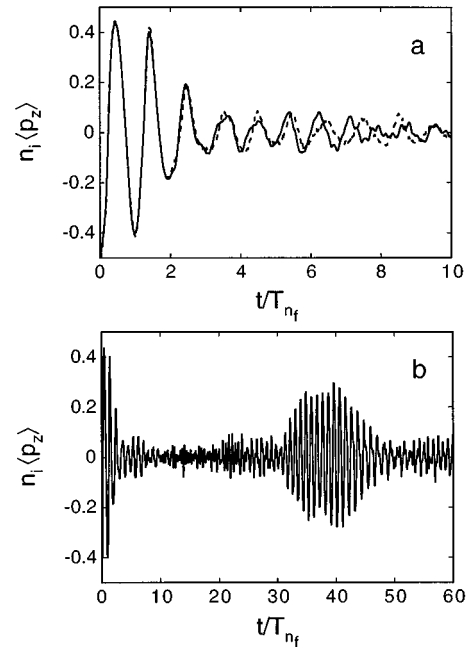

FIG. 4. Short (a) and long (b) time development (expressed in units of T_{n_f}) of the scaled expectation value $\langle p_z \rangle/p_{n_i}=n_i\langle p_z \rangle$ following application of a HCP to hydrogen atoms in the $100s$ state. The scaled momentum transfer $\Delta p/p_{n_i}=0.53$.

[1] J. A. Yeazell and C. R. Stroud, Phys. Rev. Lett. **60**, 1494 (1988); M. Mallalieu and C. R. Stroud, Phys. Rev. A **49**, 2329 (1994).

[2] B. Broers, J. F. Christian, J. H. Hoogenraad, W. J. van der Zande, H. B. van Linden van den Heuvell, and L. D. Noordam, Phys. Rev. Lett. **71**, 344 (1993).

[3] C. Raman, C. W. S. Conover, C. I. Sukenik, and P. H. Bucksbaum, Phys. Rev. Lett. **76**, 2436 (1996).

[4] R. R. Jones, D. You, and P. H. Bucksbaum, Phys. Rev. Lett. **70**, 1236 (1993).

[5] M. T. Frey, F. B. Dunning, C. O. Reinhold, and J. Burgdörfer, Phys. Rev. A **53**, R2929 (1996).

[6] C. O. Reinhold, M. Melles, and J. Burgdörfer, Phys. Rev. Lett. **70**, 4026 (1993); C. O. Reinhold, M. Melles, H. Shao, and J. Burgdörfer, J. Phys. B **26**, L659 (1993).

[7] C. O. Reinhold and J. Burgdörfer, Phys. Rev. A **51**, R3410 (1995); C. O. Reinhold, J. Burgdörfer, R. Jones, C. Raman, and P. Bucksbaum, J. Phys. B **28**, L457 (1995).

[8] P. Krstic and Y. Hahn, Phys. Rev. A **50**, 4629 (1994); C. D. Schwieters and J. B. Delos, *ibid.* **51**, 1023 (1995); A. Bugacov, B. Piraux, M. Pont, and R. Shakeshaft, *ibid.* **51**, 1490 (1995); K. J. LaGattuta and P. Lerner, *ibid.* **49**, R1547 (1994); V. Enss, V. Kostrykin, and R. Schrader, *ibid.* **50**, 1578 (1994); M. Mallalieu and S. Chu (private communication).

[9] N. E. Tielking, T. J. Bensky, and R. R. Jones, Phys. Rev. A **51**, 3370 (1995).

[10] N. E. Tielking and R. R. Jones, Phys. Rev. A **52**, 1371 (1995).

[11] M. Berry, Physica D **33**, 261 (1988).

[12] M. T. Frey, S. B. Hill, K. A. Smith, and F. B. Dunning, Phys. Rev. Lett. **75**, 810 (1995).

[13] A. Messiah, *Quantum Mechanics* (North-Holland, Amsterdam, 1967), Vol. 1.

[14] R. R. Jones, Phys. Rev. Lett. **76**, 3927 (1996).